Journal of Quantitative Spectroscopy & Radiative Transfer 111 (2010) 1980–1989

Contents lists available at ScienceDirect

Journal of Quantitative Spectroscopy & Radiative Transfer

journal homepage: www.elsevier.com/locate/jqsrt

On geometric optics and surface waves for light scattering by spheres

K.N. Liou [a], Y. Takano [a,*], P. Yang [b]

[a] Joint Institute for Earth System Science and Engineering, and Department of Atmospheric and Oceanic Sciences, University of California, Los Angeles, CA 90095, USA

[b] Department of Atmospheric Sciences, Texas A&M University, College Station, TX 77845, USA

ARTICLE INFO

Article history:
Received 14 February 2010
Received in revised form
6 April 2010
Accepted 8 April 2010

Keywords:
Geometric optics
Surface waves
Ray-by-ray tracing
Lorenz–Mie scattering

ABSTRACT

A geometric optics approach including surface wave contributions has been developed for homogeneous and concentrically coated spheres. In this approach, a ray-by-ray tracing program was used for efficient computation of the extinction and absorption cross sections. The present geometric-optics surface-wave (*GOS*) theory for light scattering by spheres considers the surface wave contribution along the edge of a particle as a perturbation term to the geometric-optics core that includes Fresnel reflection–refraction and Fraunhofer diffraction. Accuracies of the *GOS* approach for spheres have been assessed through comparison with the results determined from the exact Lorenz–Mie (*LM*) theory in terms of the extinction efficiency, single-scattering albedo, and asymmetry factor in the size–wavelength ratio domain. In this quest, we have selected a range of real and imaginary refractive indices representative of water/ice and aerosol species and demonstrated close agreement between the results computed by *GOS* and *LM*. This provides the foundation to conduct physically reliable light absorption and scattering computations based on the *GOS* approach for aerosol aggregates associated with internal and external mixing states employing spheres as building blocks.

1. Introduction

The geometric optics approach has been used to compute the angular distribution of scattered light involving interactions of a plane electromagnetic wave with a particle much larger than the incident wavelength. This approach is based on the postulation that the light beam may be thought of as consisting of separate localized rays that travel along straight-line paths; an asymptotic approximation to the exact wave equation that becomes increasingly accurate as the size parameter x approaches infinity, where x is defined as $2\pi a/\lambda$ with a the particle's radius and λ the wavelength. The physical processes of geometric optics include geometric rays externally reflected by the particle and rays refracted into the particle (see Fig. 1a), which may be absorbed in it or may undergo, in principle, an infinite number of internal reflections. The energies of a ray reflected and refracted can be evaluated by Fresnel's and Snell's laws, while the total energy scattered and absorbed by the particle is equal to that impinging on the particle's cross section perpendicular to the incident light beam.

A particle much larger than the incident wavelength also scatters light by which energy is removed from the light beam passing by the particle, referred to as diffraction, which is concentrated in a narrow lobe in the forward direction (see Fig. 1a). It contains an amount of energy equal to that incident on the particle's cross section, exactly the same as geometric reflection and refraction. The theoretical foundation of diffraction begins

* Corresponding author. Tel.: +1 310 206 4937.
E-mail address: ytakano@atmos.ucla.edu (Y. Takano).

0022-4073/$ - see front matter © 2010 Elsevier Ltd. All rights reserved.
doi:10.1016/j.jqsrt.2010.04.004

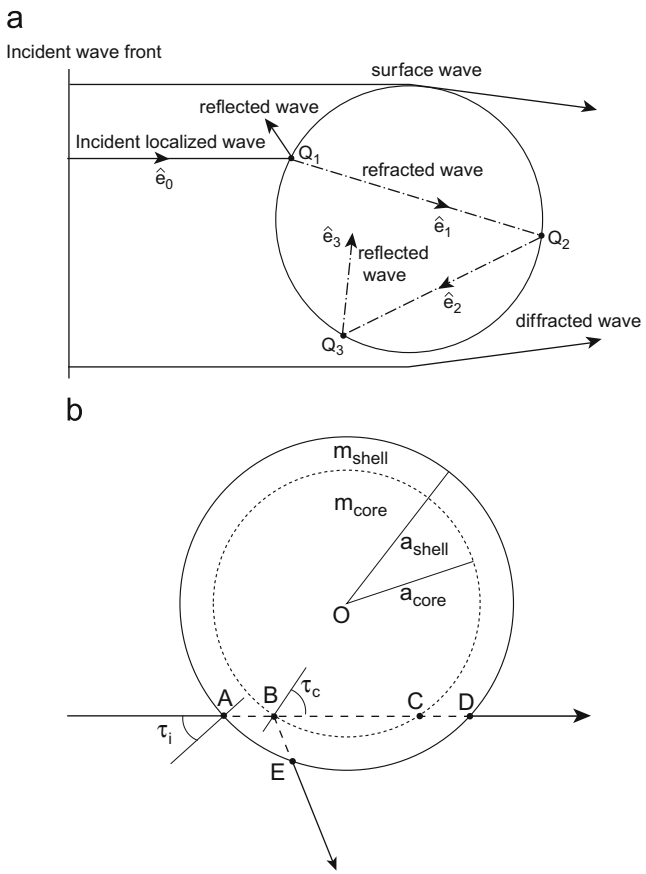

Fig. 1. (a) An illustrative geometry for a modified ray-by-ray geometric optics approach including surface wave contributions (*GOS*) for light scattering by a sphere and (b) a non-deflected ray and internally reflected ray paths involving a concentric spherical particle. The notations are defined as follows: $\hat{e}_p$ denotes a ray propagation vector; Q_p is an incident point; m_{core} and m_{shell} denote refractive indices for core and shell, and a_{core} and a_{shell} are respective radii; and τ_i and τ_c are incident angles.

with Babinet's principle, which states that the diffraction pattern in the far field, referred to as Fraunhofer diffraction, from a circular aperture is the same as that from an opaque disk or sphere of the same radius. When the size parameter is very large, the total extinction (cross section), the sum of scattering and absorption cross sections, is twice the geometric cross section area in reference to the incident beam, known as the extinction paradox [1]. Liou and Hansen [2] undertook a study to understand limitations of the geometric optics approach in the scattering phase matrix calculation for homogeneous spheres through comparison with the results computed from the exact Lorenz–Mie theory, and showed that the two methods are in close agreement when $x > 400$.

The laws of geometric optics have been extensively employed to evaluate the scattering, absorption, and polarization properties of nonspherical ice crystals, which cannot be solved by rigorous electromagnetic wave equations because it is not possible to impose suitable coordinate systems so that a variable separation method can be implemented. The geometric optics approach coupled with the Monte Carlo photon tracing has been proven to be a powerful and efficient method for light scattering and radiative transfer calculations involving ice particles [3–7]; see also the references cited in Yang and Liou [8]. The conventional geometric optics approach has fundamental limitation in its application to small size parameters, in addition to the assumption of equal partition of total incident energy between geometric reflection and refraction and Fraunhofer diffraction.

Yang and Liou [9] developed an improved geometric ray-tracing approach for the calculations of the single-scattering and polarization properties of arbitrarily oriented ice crystals in which the near field on the ice crystal surface is solved by geometric reflection and refraction. This is followed by mapping the tangential electric and magnetic currents on the particle surface to far field by means of the basic electromagnetic wave theory in three-dimensional space. In this matter, the extinction paradox in the context of geometric optics is removed and, at the same time, reliable accuracies in practical terms can be achieved for the single-scattering and phase matrix results for randomly oriented ice particles with size parameters as small as $\sim$20. The accuracy assessment was based on comparison with the results computed from a more exact numerical technique, known as the finite-difference time domain (FDTD) method [10,11].

The concept of applying the principle of geometric optics to the computation of near field on the particle surface has been reported in an early paper [12]. Yang and Liou [13] further developed a geometric optics method, referred to as the ray-by-ray (RBR) integration algorithm, which is particularly useful for the calculation of extinction and absorption cross sections for hexagonal ice crystals with size parameters as small as ~15. More recently, "exact" equations for the computations of Snell's refraction angle and Fresnel's coefficients have been derived [14,15] for large absorbing particles which take into account the inhomogeneous properties of internal waves within an absorbing particle.

In this paper, we have investigated applicability of the RBR approach to a homogeneous sphere and compared the scattering and absorption results to those computed from the exact Lorenz–Mie theory. We found substantial differences in the results between the two for all size parameters, caused by the neglect of surface waves (see Fig. 1a), which are generated by interactions of the incident waves at the grazing angles near the edge of a sphere and propagate along its surface into the shadow region [1,16]. We further applied the RBR approach coupled with surface wave contributions to spheres with layer structure for potential application to aggregate particles involving internal and external mixing states. In Section 2, we outline the physical and mathematical fundamentals of a geometric optics approach including surface wave contributions. Subsequently, we present in Section 3 a comprehensive comparison of the single-scattering properties (extinction efficiency, single-scattering albedo, and asymmetry factor) determined from the present geometric-optics surface-wave theory and the exact Lorenz–Mie results and discuss deviations between the two. Conclusions are given in Section 4.

2. Formulation of the geometric optics approach including surface wave contributions

2.1. A modified geometric optics approach

We have developed a RBR method for the computation of extinction and absorption coefficients for homogeneous and concentrically coated spheres on the basis of the approach presented in [13]. As pointed out in that paper, this RBR geometric optics method is a generalization form of the anomalous diffraction approximation (ADA) [1] and that the RBR approach reduces to ADA in optically tenuous cases. In this subsection, we should capture a number of key physical and mathematical steps involving RBR for computational purposes. Using the notations in [13], the amplitude scattering matrix $\mathbf{S}(\hat{r})$, required for single-scattering calculations, is the sum of the contributions from all localized rays as follows:

$$\mathbf{S}(\hat{r}) = \sum_{\gamma}\sum_{p}\mathbf{S}_p(\hat{r}), \tag{1}$$

where the first summation covers all the incident rays impinging onto the sphere denoted by γ, while the second summation is over the internal localized ray denoted by the subscript index p (=1, 2, 3, …), as shown in Fig. 1(a), based on the localization principle. The amplitude scattering matrix for an individual ray can be written in the form

$$\begin{aligned}\mathbf{S}_p(\hat{r}) &= \sum_q \mathbf{S}_{p,q}(\hat{r}) \\ &= \frac{k^2}{4\pi}\sum_q\left(\frac{(1-\varepsilon)}{m-\hat{r}\cdot\hat{e}_p}\mathbf{K}_p\mathbf{U}_p\boldsymbol{\Gamma}\{\exp[i\zeta_{p+1}(\hat{r})]-\exp[i\zeta_p(\hat{r})]\}\right)_q,\end{aligned} \tag{2}$$

where the phase of a ray is defined by

$$\zeta_p(\hat{r}) = k\left(\hat{e}_0\,\mathbf{r}_{Q_1} + \sum_{j=1}^{p-1} m_j d_j - \hat{r}\,\mathbf{r}_{Q_p}\right), \tag{3}$$

and m denotes an average complex refractive index in a general inhomogeneous case. For a concentrically coated sphere (see Fig. 1b), this value can be determined, for example, by the Maxwell–Garnett mixing rule [17]. The term m_j represents the complex refractive index for the inhomogeneous layer in a sphere; ε is the permittivity; k is the wavenumber; $\hat{r}$ is the scattering direction; Q_1, Q_p, and $\hat{e}_p$ are defined in Fig. 1(a); and d_j is a distance between the two points Q_j and Q_{j+1} defined by $|\mathbf{r}_{Q_{j+1}}-\mathbf{r}_{Q_j}|$. The summation over q signifies the travel of a ray through homogeneous segments of an inhomogeneous particle. Because our main objective is to effectively compute extinction and absorption cross sections, we have simplified the preceding matrix formulation by replacing the factor $\mathbf{K}_p\mathbf{U}_p\boldsymbol{\Gamma}$ by ± 1 such that the coordinate transformation for polarization denoted in Eq. (2) is neglected. Thus, the diagonal elements of the scattering matrix $\mathbf{S}_p(\hat{r})$ can then be written in the form

$$S_{jj,p}(\hat{r}) = \pm\frac{k^2}{4\pi}\sum_q\left(\frac{1-\varepsilon}{m-\hat{r}\cdot\hat{e}_p}\{\exp[i\zeta_{p+1}(\hat{r})]-\exp[i\zeta_p(\hat{r})]\}\right)_q, \tag{4}$$

where the terms $\pm$ correspond to the sign of the cumulative product of Fresnel coefficients, $t_j^2 r_j^{p-1}$; r_j can take + or − sign; and j=1 or 2, denoting parallel (1) or perpendicular (2) components.

The extinction cross section is defined by the sum of the two diagonal elements in the forward direction as follows:

$$\sigma_e = \frac{2\pi}{k^2}\mathrm{Re}[S_{11}(\hat{e}_0)+S_{22}(\hat{e}_0)], \tag{5a}$$

where $\hat{e}_0$ denotes the incident direction and the absorption cross section is given by

$$\begin{aligned}\sigma_a = \sum_{\gamma}\sum_{p=1}^{\infty}&\exp(-2k\sum_{j=1}^{p-1} m_{i,j}d_j)[1-\exp(-2km_{i,p}d_p)] \\ &\times(t_1^2 r_1^{p-1}+t_2^2 r_2^{p-1})/2,\end{aligned} \tag{5b}$$

where $m_{i,j(\text{or } p)}$ represents the imaginary part of the refractive index for an inhomogeneous sphere. Note that the absorption cross section defined in Eq. (5b) is numerically equivalent to the expression developed for the conventional geometric optics approximation [6,18].

For a spherical particle, Eq. (4) is evaluated as if the path of twice refracted ray (p=1) were not deflected at all

such that the phase of a ray in Eq. (4) is given by

$$\zeta_2 = 2ka\cos\tau_i(m-1). \tag{6a}$$

This term is the dominant exponential term for extinction in Eq. (4), where τ_i is the incident angle and a is the radius of a sphere. Note that $\zeta_1=1$, and ζ_p $(p>2)$ terms vanish due to phase cancellation. For a sphere with layer structure, we must formulate ζ_2 to account for internal inhomogeneity. When $\sin\tau_i$ is larger than a_{core}/a_{shell}, as shown in Fig. 1(b), a ray propagating without being deflected does not intersect the inner sphere so that the ray's phase is given by

$$\zeta_2 = 2ka_{shell}\cos\tau_i\,(m_{shell}-1). \tag{6b}$$

If a_{shell} and m_{shell} are replaced by a and m, respectively, Eq. (6b) is exactly the same as Eq. (6a). In the case when $\sin\tau_i \le a_{core}/a_{shell}$, a ray intersects the inner sphere so that two split rays occur due to internal reflection between the boundaries of inner and outer spheres. In this case, ζ_2 can be expressed as follows:

$$\zeta_2 = (1-r)\zeta_{21} + r\zeta_{22}, \tag{6c}$$

where $r=(|r_l|^2+|r_r|^2)/2$, and r_l and r_r are Fresnel reflection coefficients when the incident angle τ_c is $\sin^{-1}\{\sin\tau_i/(a_{core}/a_{shell})\}$. Considering the path lengths AB, BC, and CD denoted in Fig. 1(b), the phase of a transmitted ray can be expressed as

$$\zeta_{21} = 2k[(a_{shell}\cos\tau_i - a_{core}\cos\tau_c)m_{shell} + a_{core}\cos\tau_c\cdot m_{core} - a_{shell}\cos\tau_i], \tag{7a}$$

while for an internally reflected ray (defined by AB and BE), the particle's phase is given by

$$\zeta_{22} = k\{(a_{shell}\cos\tau_i - a_{core}\cos\tau_c)[1+\cos(\pi-2\tau_c)](m_{shell}-1)\}. \tag{8}$$

The conventional geometric optics approach [6,18] can be employed for calculation of the asymmetry factor for homogeneous and layer spheres, which in combination with known extinction and absorption coefficients will be used to evaluate a term referred to as radiation pressure [1] in conjunction with the discussion presented in subsection 2.2. Light rays can carry momentum as well as energy. The part of the forward momentum that is removed from incident rays, which is not represented by the forward momentum associated with scattered rays, is related to the hemispheric average of the phase function weighted by $\cos\theta$, where θ denotes the zenith angle in the Cartesian coordinates. This term is referred to as the asymmetry factor. We can express the radiation pressure term as follows:

$$Q_{pr}(GO) = Q_{ext}(GO) - g(GO)[Q_{ext}(GO) - Q_{abs}(GO)], \tag{9}$$

where g represents the asymmetry factor, $Q_{ext}(=\sigma_e/\pi a^2)$ is the extinction efficiency, $Q_{abs}(=\sigma_a/\pi a^2)$ is the absorption efficiency, and the index GO denotes the terms evaluated by the geometric optics approach.

2.2. Surface wave adjustment (the edge effect)

For a spherical particle, the extinction and absorption efficiencies and radiation pressure evaluated from the geometric optics approach generally deviate from the results computed from the exact Lorenz–Mie theory, due principally to the neglect of surface waves along the edge of a spherical particle. These waves are produced by means of interaction of the incident waves at grazing angles near the edges of a sphere and continuation of the wave motion along its surface into the shadow region. If the sphere is relatively small, the waves may move around and encompass the entire spherical surface.

Nussenzveig and Wiscombe [16, hereafter referred to as NW] in their pioneering work, presented physical equations for the calculation of surface waves based on the complex angular momentum theory. This theory makes use of the transformation of the Debye expansion of two scattering functions in a complex domain, allowing the mapping of localized incident rays into a complex domain such that the Airy integral can be incorporated in analysis. In the following, we should capture key elements in the contribution of surface waves to light scattering processes.

The surface wave term for extinction in order of the size parameter x can be written in the form

$$\Delta Q_{ext} = c_1 x^{-2/3} + 2\mathrm{Im}[(m^2+1)(m^2-1)^{-1/2}]x^{-1} - c_2 x^{-4/3} - c_3\mathrm{Im}[e^{i\pi/3}(m^2-1)^{-3/2}(m^2+1)(2m^4-6m^2+3)]x^{-5/3}, \tag{10}$$

where $c_1=1.99239$, $c_2=0.71535$, $c_3=0.66413$, and Im denotes the imaginary part of the term (after NM with modification). The size parameter appears in the denominator of Eq. (10). For this reason, ΔQ_{ext} diverges when x approached small values and specific corrections must be made to ensure its physical continuity (see below for further discussion).

The surface wave contribution to the absorption coefficient is governed by the following two integrations:

$$\Delta Q_{abs} = 2^{-1/3}x^{-2/3}\sum_{l=1}^{2}\left\{\int_0^{y_a}\varphi(r_{jl}^{+})\,dy + \int_0^{y_b}[\varphi(r_{jl}^{-}) - \varphi(\tilde{r}_{jl}^{-})]\,dy\right\}, \tag{11}$$

where l denotes two polarization components and definitions of all the terms and integration limits are listed in the Appendix.

The radiation pressure term, which is required for calculation of the asymmetry factor for a spherical particle, is also defined by two integrations as follows:

$$\Delta Q_{pr} = -2^{-1/3}x^{-2/3}\mathrm{Re}\sum_{l=1}^{2}\left\{\int_0^{y_a}(\rho_l^{+} - \tau_l^{+} + 1)\,dy + \int_0^{y_b}[(\rho_l^{-} - \hat{\rho}_l^{-}) - (\tau_l^{-} - \hat{\tau}_l^{-})]\,dy\right\}. \tag{12}$$

where Re denotes the real part of the term and all parameters are also defined in the Appendix. This term is generally negative.

A combination of the geometric optics term and the surface wave adjustment (denoted by GOS) should, in principle, constitute a solution close to the exact solution derived from the exact Lorenz–Mie theory (denoted by LM) such that

$$Q_w(GOS) = Q_w(GO) + \Delta Q_w \approx Q_w(LM),\ \ w = ext,\ abs,\ \text{or}\ pr, \tag{13}$$

where linearity between geometric optics (*GO*) and surface wave (Δ) terms is implicitly applied. Moreover, based on Eq. (9), the asymmetry factor can be written in the form

$$g(GOS)=\frac{Q_{ext}(GOS)-Q_{pr}(GOS)}{Q_{ext}(GOS)-Q_{abs}(GOS)}. \tag{14}$$

As noted previously, because the size parameter x appears in the denominator in the right-hand side of Eq. (10), ΔQ_{ext} breaks down when x approaches zero. To investigate applicability of the surface wave term derived from the complex angular momentum theory, we have conducted analysis of ΔQ_{ext} in terms of the phase shift parameter, a function of both refractive index and size parameter, defined by

$$\rho=2|m-1|x. \tag{15}$$

The surface wave adjustment term ΔQ_{ext} (normally on the order of 0.1) approaches an unrealistic large number (a factor of more than 10) when $\rho\sim 2.86$. Additionally, we also found that the extinction efficiency results computed from the RBR geometric optics approach outlined above, without including the surface wave effect, match closely with those determined from the exact *LM* theory when $\rho<2.86$ so that surface wave adjustments are not required in this region.

3. Computational results and discussion

We have conducted a series of comparisons between the extinction efficiency, the single-scattering albedo (the ratio of the scattering efficiency to the extinction efficiency), and the asymmetry factor determined from *GOS*, and those computed from the *LM* equations for homogeneous spheres with size parameters up to 100 [19]. Note that the scattering efficiency $Q_{sca}=Q_{ext}-Q_{abs}$. A range of real refractive indices (m_r) have been selected for

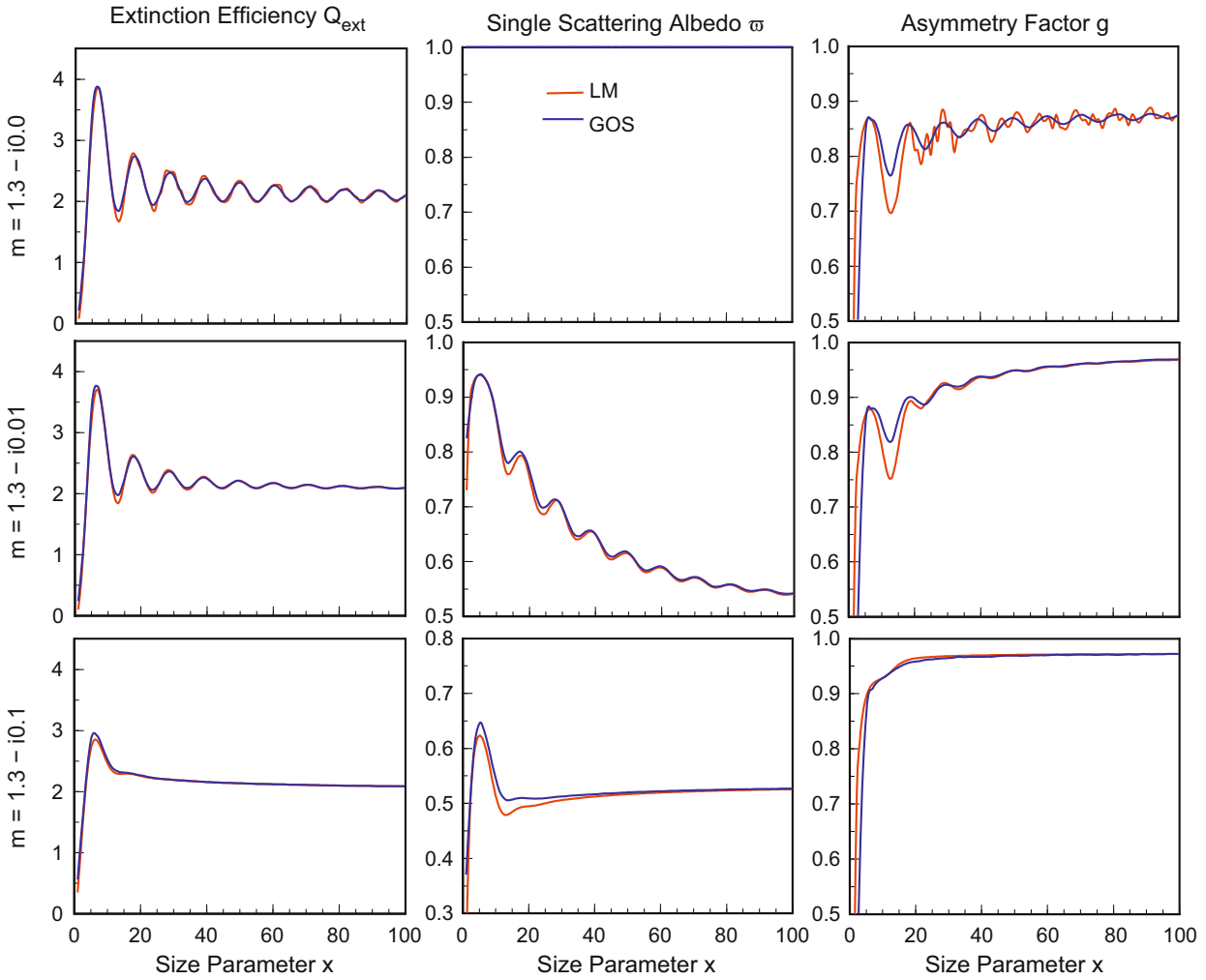

Fig. 2. Comparison of the extinction efficiency, the single-scattering albedo, and the asymmetry factor between the results computed from the Lorenz–Mie (*LM*) theory and the present geometric-optics surface-wave (*GOS*) approach for a real refractive index of 1.3 coupled with three imaginary parts of 0.0, 0.01, and 0.1. The solid (red) and dashed (blue) curves denote *LM* and *GOS*, respectively.

this purpose including 1.3, 1.5, 1.7, and 2 coupled with imaginary parts (m_i) of 0.0, 0.01, 0.1, and 1. Only selected results will be presented.

Fig. 2 displays comparison results as a function of size parameter for cases involving 1.3 and three imaginary parts indicated in the figure, representing the general optical properties of water and ice. Both the extinction efficiency and single-scattering albedo values computed from *GOS* compare remarkably well with those from the exact *LM*. Without absorption, the extinction efficiency and asymmetry factor curves display major maximum and minimum oscillations [20] as a result of wave interferences. As absorption increases (m_i=0.01 and 0.1), fluctuations are damped and for the latter case, only a single peak exists in the extinction efficiency and single-scattering albedo curves. Fig. 3 displays the results for a real refractive index of 1.5 coupled with three imaginary parts depicted in the figure, representing the general aerosol optical properties. As the real index of refraction increases from 1.3 to 1.5, oscillations increase more frequently and their strengths enhance for size parameters less than about 20. The *GOS*'s extinction results at $x\sim5$ are slightly smaller than those from *LM*. Again, as absorption increases, all the oscillations are damped, except the one located at about $x\sim5$.

Fig. 4 illustrates cases with a real refractive index of 2 coupled with imaginary parts of 0.01, 0.1, and 1, which could represent the optical properties of soot and the type of aerosols with larger absorption. In comparison with the results shown in Figs. 2 and 3, the amplitude and frequency of oscillations for extinction substantially increase when m_r=2. The amplitudes of extinction involving osillations for $x<10$ computed from *GOS* are less intense as compared to those from *LM*. For the case of m_i=1, there is only one extinction peak at $x\sim3$. Although the extinction efficiency is smaller in *GOS*, the single-scattering albedo results closely agree with those calculated from *LM*. For the asymmetry factor, deviations are shown at $x<5$ due to small contributions from the surface wave component. We have also

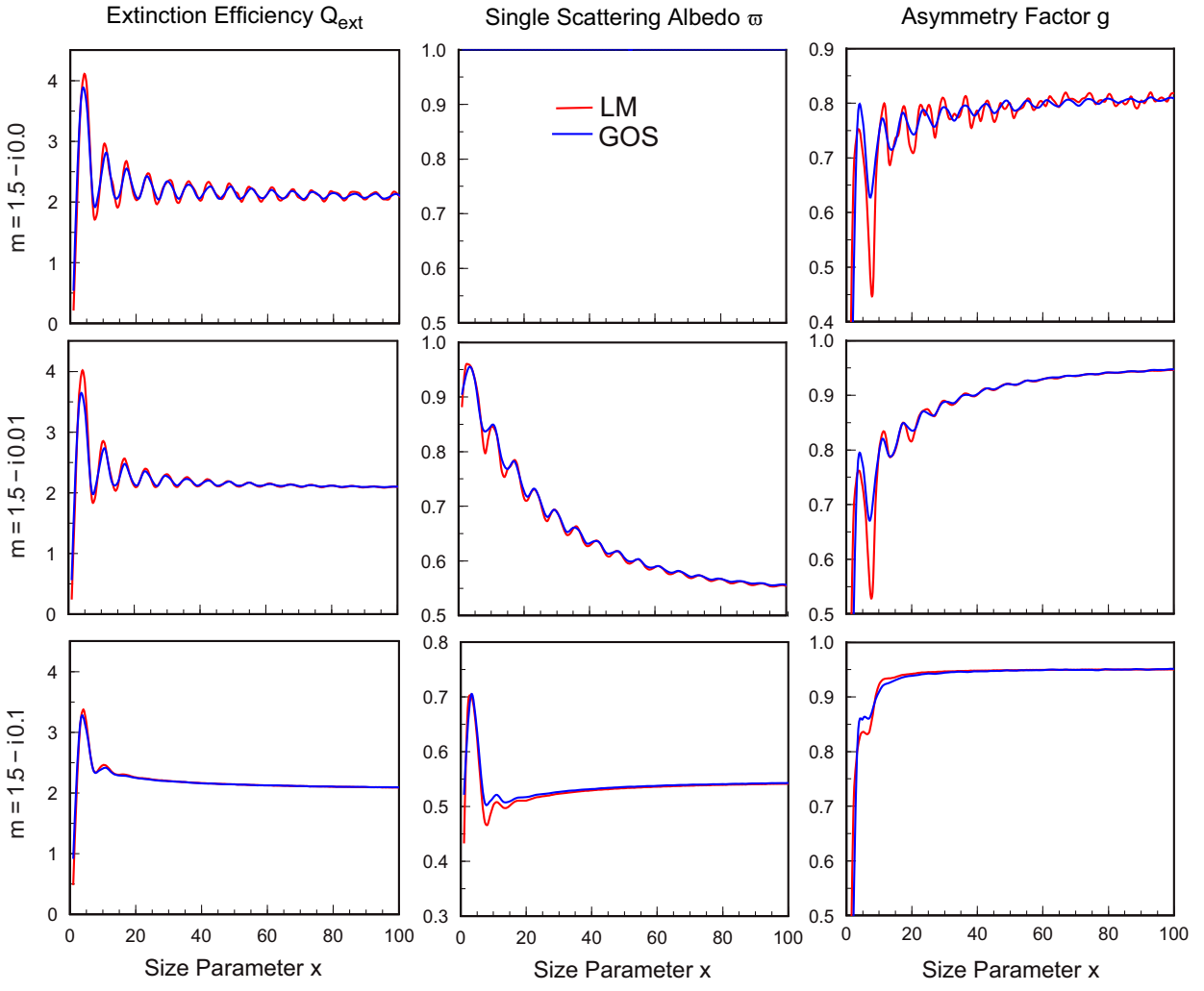

Fig. 3. Same as in Fig. 2, except that the real refractive index is 1.5.

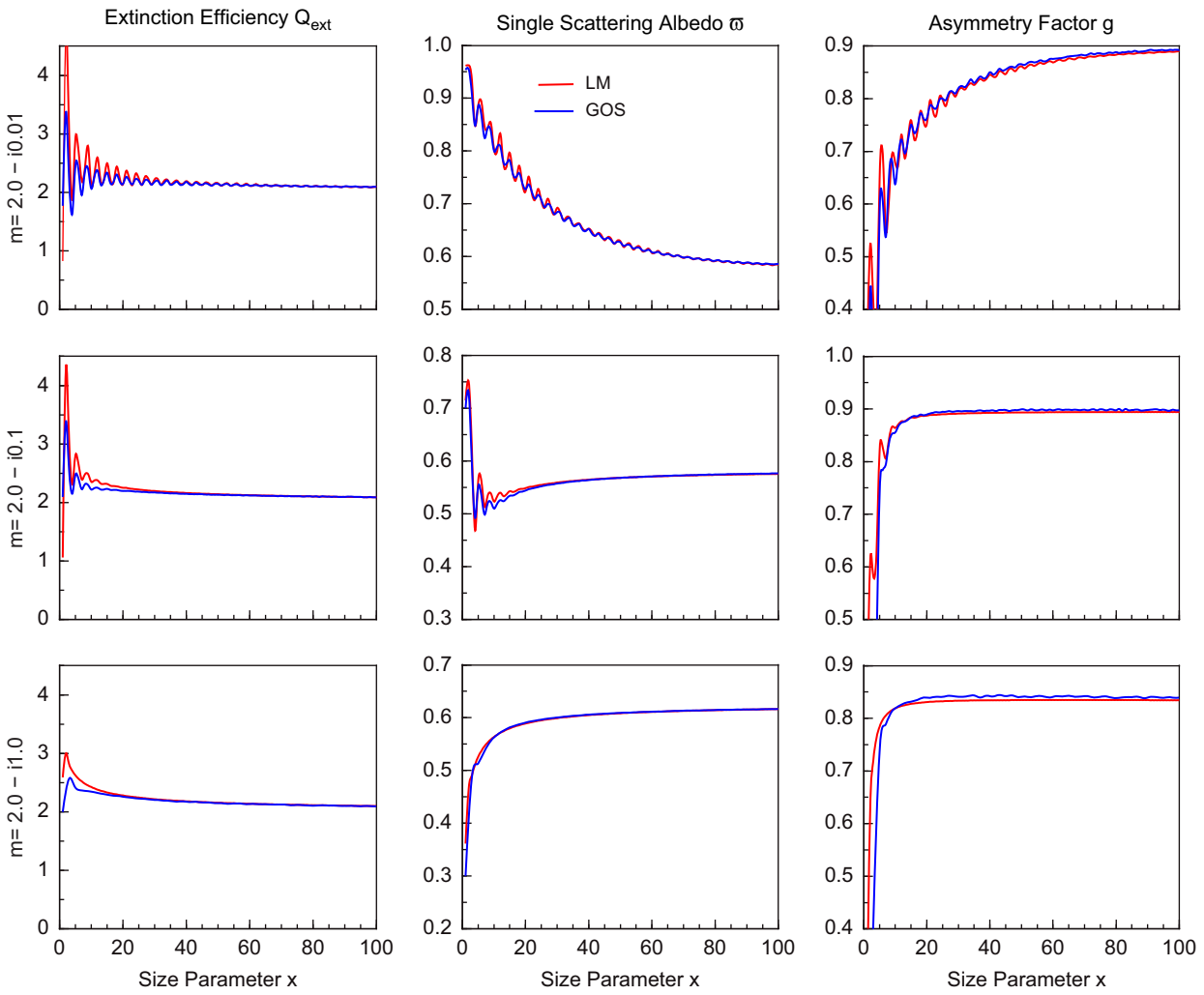

Fig. 4. Comparison of the extinction efficiency, the single-scattering albedo, and the asymmetry factor between the results computed from the Lorenz–Mie (*LM*) theory and the present geometric-optics surface-wave (*GOS*) approach for a real refractive index of 2 coupled with three imaginary parts of 0.01, 0.1, and 1.0. The solid (red) and dashed (blue) curves denote *LM* and *GOS*, respectively.

performed computations for m_r=1.7 with m_i=0.0, 0.01, and 0.1; the results of which are in between m_r=1.5 and 2, and thus are not shown here.

We have applied the *GOS* approach to cases involving concentrically coated spheres and compared the resulting single-scattering properties to those computed by the theoretical expressions presented in [21,22] on the basis of the equations developed in [23]. In [21], numerically stable algorithms for the spherical Bessel functions in the Lorenz–Mie solution were developed. For illustration purposes, we have selected three cases. In the first case (Case a), which involves non-absorption aerosols coated by water, we use m_r(core)=1.5 and m_r(shell)=1.3, along with the relative dimension of $a_{12}=a_{core}/a_{shell}$=0.8. The second case (Case b, dust coated by water) involves m(core)=1.53−0.008i and m_r(shell)=1.33 with a_{12}=0.8. The third case includes soot coated by nonabsorbing aerosols (Case c), which employs m(core)=2.0−1.0i and m_r(shell)=1.5 with a_{12}=0.2.

Fig. 5 shows comparison results for the preceding three cases computed by *GOS* and the analytical *LM*-like solution [21], referred to as *"Exact"*. In Case a, which corresponds to no absorption, we see an overall agreement between the two for the extinction efficiency and the asymmetry factor. Similar to the homogeneous cases displayed in Figs. 2 and 3, the *GOS* approach shows smaller amplitudes in oscillations. In Case b, absorption substantially enhances as the size parameter increases because core radius is relatively large (80% of the shell). The single-scattering albedo values ranging from ∼0.9 (x∼10) to ∼0.6 (x∼100) computed from the *"Exact"* and *GOS* approaches appear to compare quite well. The asymmetry factor curves display differences between the two results at x∼7 (minimum) and x∼10 (maximum). Regarding Case c, absorption by dark soot (20% of the shell) shows that the single-scattering albedo values fluctuate around ∼0.9 with slight deviations between the two methods. Except the

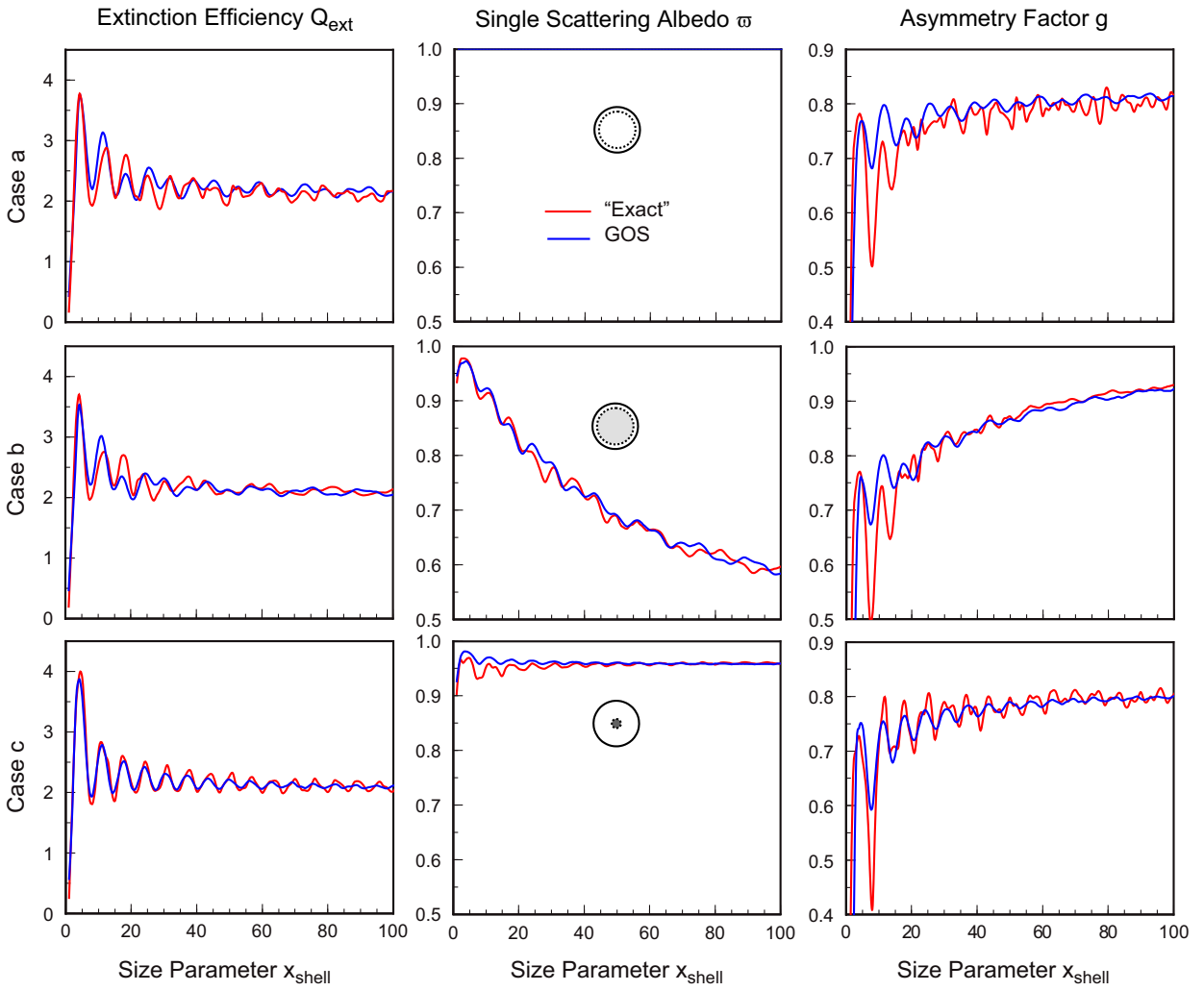

Fig. 5. Comparison of the extinction efficiency, the single-scattering albedo, and the asymmetry factor between the results computed from the Lorenz–Mie like solution (*"Exact"*) and the present geometric-optics surface-wave (*GOS*) approach for three cases of concentrically coated spheres. Case a (upper panel): m_r(core)=1.5, m_r(shell)=1.33, and the relative dimension $a_{12}=a_{core}/a_{shell}=0.8$. Case b (middle panel): m(core)=1.53 − 0.008i, m_r (shell)=1.33, and $a_{12}=0.8$. Case c (lower panel): m(core)=2 − 1.0i, m_r(shell)=1.5, and $a_{12}=0.2$. The solid (red) and dashed (blue) curves denote *"Exact"* and *GOS*, respectively.

minimum located at $x\sim 8$, the asymmetry factor values appear to be in close agreement between the two approaches.

4. Conclusions

In this paper, we have developed a geometric optics approach including the contribution from surface waves for homogeneous spheres and spheres with layer structure. In this development, we modified the ray-by-ray approach [13], which is particularly useful for the computation of extinction and absorption cross sections for a particle composed of a spherical core surrounded by a concentric shell. This geometric-optics surface-wave theory for light scattering by spheres considers the surface wave contribution as a perturbation term to the geometrics optics core that includes Fresnel reflection–refraction and Fraunhofer diffraction. For surface wave contributions, we followed the analytical expressions derived for the terms involving the extinction and absorption cross sections and radiation pressure on the basis of the complex angular momentum theory [16]. We specifically focused on the calculations of three basic parameters: extinction efficiency, single-scattering albedo, and asymmetry factor. The last parameter is related to the radiation pressure term [1].

Reliability and accuracy of the present geometric-optics surface-wave (*GOS*) approach have been assessed by comparison with the results determined from the Lorenz–Mie (*LM*) theory. For homogeneous spheres, we have selected a range of real (1.33–2.0) and imaginary (0.0–1.0) refractive indices in association with water/ice and aerosol species. We demonstrated that the extinction efficiency, single-scattering albedo, and asymmetry factor

results computed by *GOS* and *LM* are in close agreement for a combination of aforementioned real-imaginary refractive indices as functions of size parameter. The oscillations in the single-scattering properties for larger real refractive indices (e.g., m_r=2) and size parameters smaller than about 20 generated by *GOS* are less intense as those produced by the exact *LM* theory.

The *GOS* approach was further applied to spheres composed of a spherical core and a shell with a number of real and imaginary refractive indices and size combinations. We assessed the resulting computations with those evaluated from the efficient algorithms presented in [21] based on the analytical *LM* solution for spherical core–shell structure, and demonstrated the same order of accuracy as in the cases involving homogeneous spheres. The close agreement between *GOS* and the *"Exact" LM*-like solution provides the foundation to conduct physically reliable light absorption and scattering for aerosol aggregates with internal and external mixing, which can be built from homogeneous and inhomogeneous spheres.

Acknowledgments

This study was supported in part by the National Science Foundation under Grant ATM-0331550.

Appendix

The surface wave term for absorption efficiency defined in Eq. (11) contains a function φ given by

$$\varphi(r_{jl}) = (1-e^{-b})(1-r_{2l})/(1-r_{1l}e^{-b}), \tag{A1}$$

where r_{2l} and r_{1l} are, respectively, the external and internal reflectivities for polarization l, which are given by

$$r_{jl} = |R_{jl}|^2, \quad j,l = 1,2; \quad R_{j,l} = (-1)^j(z_j - ue_l)/(z + ue_l), \tag{A2}$$

$$z = \cos\theta,\ u = m\cos\theta',\ \sin\theta = m\sin\theta',\ e_1 = 1,\ e_2 = m^{-2},\ z_1 = z,\ z_2 = z^*, \tag{A3}$$

where z^* denotes the complex conjugate of z and $b = 4x\mathrm{Im}(m\cos\theta' + \theta'\sin\theta)$. The term $r_{jl}^{\pm}$ in Eq. (11) is obtained from r_{jl} such that z is replaced by

$$z^{\pm} = -(2/x)^{1/3}e^{i\pi/6}\mathrm{Ai}'(\pm ye^{2i\pi/3})/\mathrm{Ai}(\pm ye^{2i\pi/3}), \tag{A4}$$

where Ai is the Airy function, prime signifies derivative, and θ is related to y by

$$\sin\theta = 1 \pm 2^{-1/3}x^{-2/3}y, \tag{A5}$$

where the + and − signs apply to the first and second integrals in Eq. (11), respectively. The integration limits are given by

$$y_a = 2^{1/3}(m-1)x^{2/3}, \quad y_b = (x/2)^{2/3}. \tag{A6}$$

The term $\tilde{r}_{jl}^{-}$ is obtained from r_{jl}^{-} such that z^- is replaced by $(2/x)^{1/3}y^{1/2}$.

The surface wave term for radiation pressure ΔQ_{pr} in Eq. (12) contains the following terms:

$$\rho_l = f_1(z)R_{2l}{}^*R'_{2l}, \tag{A7}$$

$$\tau_l = f_1(z)f_2e^{-b}(1+R_{1l}{}^*)(1+R'_{1l})(1+R_{2l}{}^*)(1+R'_{2l}) \times (1+R_{1l}{}^*R'_{1l}f_2e^{-b})^{-1}, \tag{A8}$$

$$R'_{j1} = (f_j)^{-1}[m^2z_j - u + (-1)^j iM^2](m^2z + u + iM^2)^{-1}, \tag{A9}$$

$$R'_{j2} = (f_j)^{-1}[(m^2+M^2)z_j - u + (-1)^j iM^2(1-uz_j)] \times [(m^2+M^2)z + u + iM^2(1+uz)]^{-1}, \tag{A10}$$

$$f_1(z) = (1+iz^*)/(1-iz), \quad f_2 = e^{-2i\theta'}, \tag{A11}$$

with $M^2 = m^2 - 1$. In all the parameters with $\pm$ upper indices defined in Eq. (12) in the text, substitutions denoted by Eqs. (A5) and (A6) are required. The terms $\hat{\rho}_l^-$ and $\hat{\tau}_l^-$ are obtained from ρ_l^- and τ_l^- such that z^- is replaced by $(2/x)^{1/3}(\sqrt{y} + i/4y)$. Note that the preceding equations are modifications based on those presented in [16].

References

[1] van de Hulst HC. Light Scattering by Small Particles. New York: Wiley; 1957.
[2] Liou KN, Hansen JE. Intensity and polarization for single scattering by polydisperse spheres: a comparison of ray optics and Mie theory. J Atmos Sci 1971;28:995–1004.
[3] Wendling P, Wendling R, Weickmann HK. Scattering of solar radiation by hexagonal ice crystals. Appl Opt 1979;18:2663–71.
[4] Liou KN, Coleman RF. Light scattering by hexagonal columns and plates. In: Schuerman DW, editor. Light Scattering by Irregularly Shaped Particles. New York: Plenum Publishing Corporation; 1980. p. 207–18.
[5] Cai QM, Liou KN. Theory of polarized light scattering by hexagonal ice crystals. Appl Opt 1982;21:3569–80.
[6] Takano Y, Liou KN. Solar radiative transfer in cirrus clouds. Part I: single-scattering and optical properties of hexagonal ice crystals. J Atmos Sci 1989;46:3–19.
[7] Macke A. Scattering of light by polyhedral ice crystals. Appl Opt 1993;32:2780–8.
[8] Yang P, Liou KN. Light scattering and absorption by nonspherical ice crystals. In: Alexander Kokhanovsky, editor. Light Scattering Reviews: Single and Multiple Light Scattering. London: Springer, PRAXIS Publishing Ltd.; 2006. p. 31–71.
[9] Yang P, Liou KN. A geometric-optics/integral-equation method for light scattering by nonspherical ice crystals. Appl Opt 1996;35:6568–84.
[10] Muinonen K. Scattering of light by crystals: a modified Kirchhoff approximation. Appl Opt 1989;28:3044–50.
[11] Yee SK. Numerical solution of initial boundary value problems involving Maxwell's equations in isotropic media. IEEE Trans Antennas Propag 1966;14:302–7.
[12] Yang P, Liou KN. Finite-time domain method for light scattering by small ice crystals in three-dimensional space. J Opt Soc Am A 1996;13:2072–85.
[13] Yang P, Liou KN. Light scattering by hexagonal ice crystals: solution by a ray-by-ray integration algorithm. J Opt Soc Am A 1997;14:2278–89.
[14] Yang P, Liou KN. Effective refractive index for determining ray propagation in an absorbing dielectric particle. JQSRT 2009;110:300–6.
[15] Yang P, Liou KN. An "exact" geometric optics approach for computing the optical properties of large absorbing particles. JQSRT 2009;110:1162–77.
[16] Nussenzveig HM, Wiscombe WJ. Efficiency factor in Mie scattering. Phys Rev Lett 1980;45:1490–4.
[17] Chylek P, Ramaswamy V, Chen RJ. Effect of graphitic carbon on the albedo of clouds. J Atmos Sci 1984;41:3076–84.

[18] Takano Y, Liou KN. Radiative transfer in cirrus clouds. III. Light scattering by irregular ice crystals. J Atmos Sci 1995;52:818–37.
[19] Takano Y, Tanaka M. Phase matrix and cross section for single scattering by circular cylinders: a comparison of ray optics and wave theory. Appl Opt 1980;19:2781–93.
[20] Liou KN. An Introduction to Atmospheric Radiation. San Diego: Academic Press; 2002.
[21] Toon OB, Ackerman TP. Algorithms for the calculation of scattering by stratified spheres. Appl Opt 1981;20:3657–60.
[22] Ackerman TP, Toon OB. Absorption of visible radiation in atmosphere containing mixtures of absorbing and nonabsorbing particles. Appl Opt 1981;20:3661–6.
[23] Kerker M. The Scattering of Light and Other Electromagnetic Radiation. New York: Academic Press; 1969.